Supplementary Information for

Vinylboronic acid pinacol ester as a vinyl alcohol-precursor monomer in radical copolymerizations with styrene

Hiroshi Makino, Tsuyoshi Nishikawa* and Makoto Ouchi*

Department of Polymer Chemistry, Graduate School of Engineering, Kyoto University, Kyoto 615-8510, Japan

*To whom correspondence should be addressed.

E-mail: nishikawa.tsuyoshi.8n@kyoto-u.ac.jp
ouchi.makoto.2v@kyoto-u.ac.jp

Contents

1 General

All reactions were carried out with magnetic stirring under nitrogen or argon atmosphere unless otherwise stated. ^{1}H NMR spectra were recorded on a JEOL JNM-ECA500 operating at 500.16 MHz at ambient temperature and the data are recorded on the basis of the chemical shift in ppm downfield from tetramethylsilane (δ scale). IR spectra were obtained using an Agilent Technologies Cary 630 FTIR spectrometer. The number-average molar mass (M_n) and M_w/M_n ratio of polymers were measured by size exclusion chromatography (SEC) at 40 °C in THF as an eluent on two polystyrene-gel columns (Shodex LF-404). The columns were calibrated against standard polystyrene samples (TOSOH TSK Standard). Preparative SEC-based polymer purification was performed using JAIGEL-2.5HR or Shodex KF-5001 columns ($CHCl_3$). For the purification by dialysis, MWCO1000 (Spectra/PorVR7, diameter 11.5 mm) was used as the dialysis tubing. Thermal properties of polymers were measured by differential scanning calorimetry (DSC) with ca. 3-5 mg of sample (in aluminum pan) under dry nitrogen flow on DSCQ200 calorimeter (TA Instruments) equipped with RCS 90 electric freezing machine. The sample was heated and cooled at 10 ˚C/min between –30 ˚C and 150 ˚C, and the glass transition temperature (T_g) was evaluated on the second heating process.

Vinylboronic acid pinacol ester (VBpin), methyl methacrylate (MMA), methyl acrylate (MA), styrene (St), acrylonitrile (AN), 4-methoxystyrene (PMOS), 4-chlorostyrene (4CS) and tetralin were purified by distillation prior to use. Azobisisobutyronitrile (AIBN), 2-cyano-2-propyl dodecyl trithiocarbonate (CPDT), aqueous hydrogen peroxide (30wt%), sodium hydroxide, dehydrated toluene and ethanol were purchased from the commercial sources and were used without further purification.

2 Experimental Procedures

Free radical copolymerization of VBpin with common vinyl monomers

The copolymerization was performed in toluene at 60 ˚C with AIBN as an initiator under inert gas atmosphere; $[VBpin]_0 = [comonomer]_0 = 1$ M, $[AIBN]_0 = 20$ mM. The typical procedure for the copolymerization (comonomer: styrene) is as follows: A toluene solution of AIBN (493 μL, 4.9 mg, 30 μmol) was placed in a Schlenk tube with a PTFE stopcock (J. Young) under Ar atmosphere. Tetralin (40.9 μL, 39.7 mg, 300 μmol, internal standard), VBpin (257 μL, 231 mg, 1.50 mmol), St (172 μL, 156 mg, 1.5 mmol) and toluene (538 μL) were then added at room temperature. The reaction mixture was stirred at 60 °C in an oil bath. The conversions of both monomers were monitored by ^{1}H NMR: Conv. (VBpin) = 24%, Conv. (St) = 75% in 72 hours. The solution was evaporated, followed by SEC analysis for determination of M_n and M_w/M_n of the resultant copolymer: $M_n = 7.8 \times 10^3$, $M_w/M_n = 1.73$. Copolymerization with other vinyl monomers were also performed similarly.

RAFT copolymerization of VBpin with St in the presence of CPDT

The RAFT copolymerization was performed in toluene at 60 ˚C with AIBN as an initiator and CPDT as a CTA under inert gas atmosphere; $[VBpin]_0 = [St]_0 = 2$ M, $[CPDT]_0/[AIBN]_0 = 0.8$. The typical procedure for the RAFT polymerization $[([VBpin]_0+[St]_0)/[CPDT]_0 = 100]$ is as follows: AIBN (3.94 mg 24.0 μmoL), tetralin (40.9 μL, 39.7 mg, 300 μmol, internal standard), CPDT (10.5 μL, 10.4 mg, 30.0 μmol), VBpin (257 μL, 231 mg, 1.50 mmol), St (172 μL, 156 mg, 1.50 mmol), and toluene (270 μL) were placed in a Schlenk tube with PTFE stopcock (J. Young) at room temperature under Ar atmosphere. The reaction mixture was stirred at 60 °C in an oil bath. The conversions of both monomers and the molar mass of resulting polymer were monitored by ^{1}H NMR and SEC: Conv. (VBpin) = 50%, Conv. (St) = 88%, $M_n = 5.0 \times 10^3$, $M_w/M_n = 1.43$. in 72 hours. Copolymerization in the different monomer CTA ratio $[([VBpin]_0+[St]_0)/[CPDT]_0 = 200, 400]$ were also performed similarly.

Typical procedure for synthesis of poly(VA-*co*-St) through oxidation

The polymer obtained in copolymerization of VBpin and St was purified by preparative SEC to remove the remained monomers. The obtained poly(VBpin-*co*-St)

(100 mg) was dissolved in THF (28.3 mL). Ethanol (3.0 mL), an aqueous solution of NaOH (6 M, 3.0 mL), and an aqueous solution of H_2O_2 (35wt%, 6.0 mL) were added. The reaction solution was stirred at room temperature under air. After 24 h, the reaction solution was neutralized using HCl aq. The volume of the solution was reduced to 20 mL by evaporation. The dialysis was repeated with varying the solvent (water/THF = 50/50 (v/v) → water/THF = 30/70 → THF). After evaporation, the residue was purified by preparative SEC. Finally, poly(vinyl alcohol-*co*-styrene) (poly(VA-*co*-St)) was obtained as a colorless solid (61 mg). The purification process was modified depending on the polarity of resulting copolymer, and it was summarized in Table

3 Results of Free Radical Copolymerization

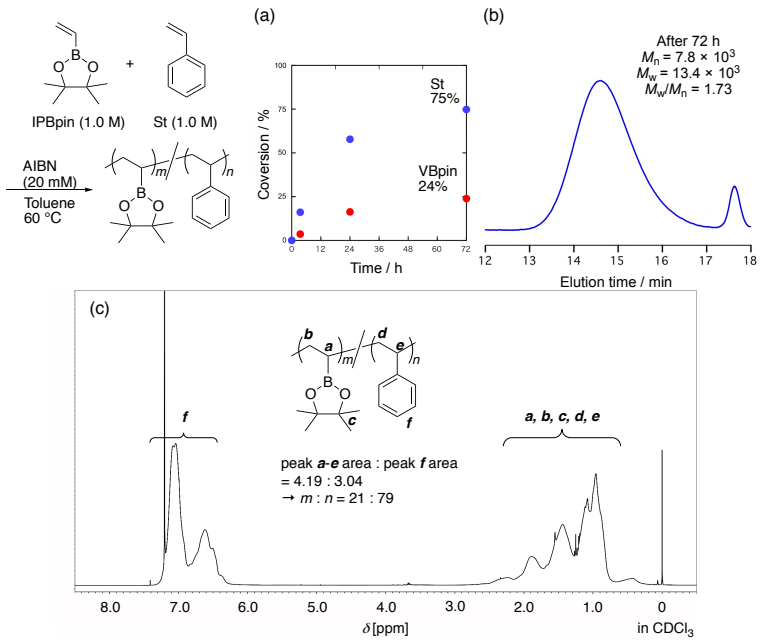

Figure S1. Radical copolymerization of VBpin with St: (a) Time-conversion curves, (b) SEC trace of the resulting copolymer, (c) ^{1}H NMR spectrum of poly(VBpin-*co*-MA) in $CDCl_3$ after the purification.

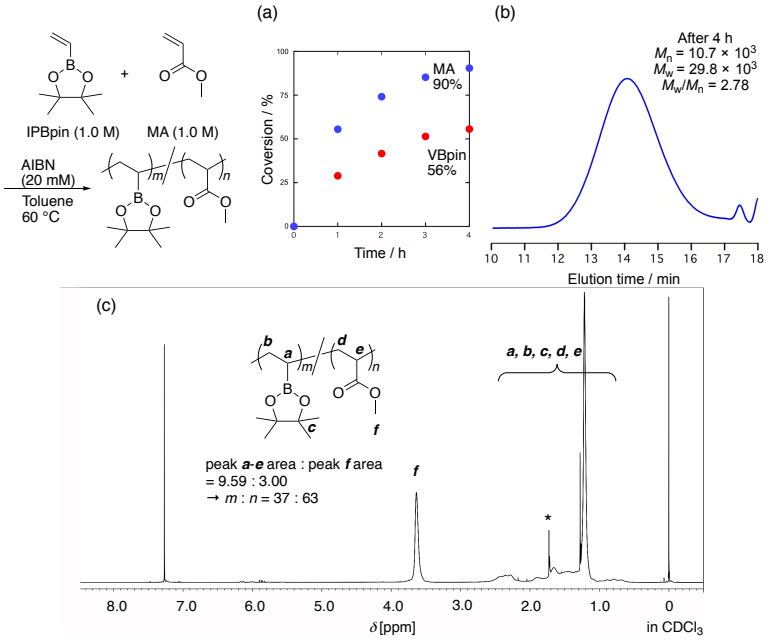

Figure S2. Radical copolymerization of VBpin with MA: (a) Time-conversion curves, (b) SEC trace of the resulting copolymer, (c) ^{1}H NMR spectrum of poly(VBpin-*co*-MA) in $CDCl_3$ after the purification.

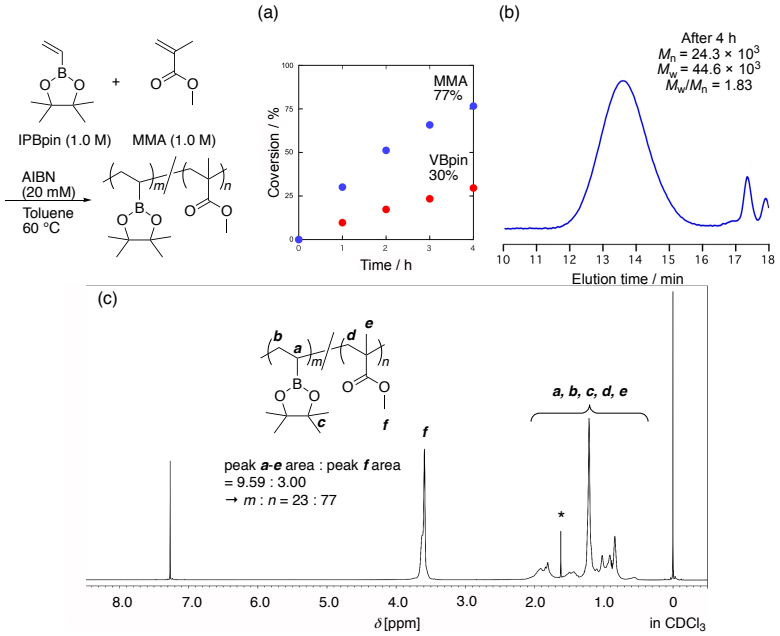

Figure S3. Radical copolymerization of VBpin with MMA: (a) Time-conversion curves, (b) SEC trace of the resulting copolymer, (c) ^{1}H NMR spectrum of poly(VBpin-*co*-MMA) in $CDCl_3$ after the purification.

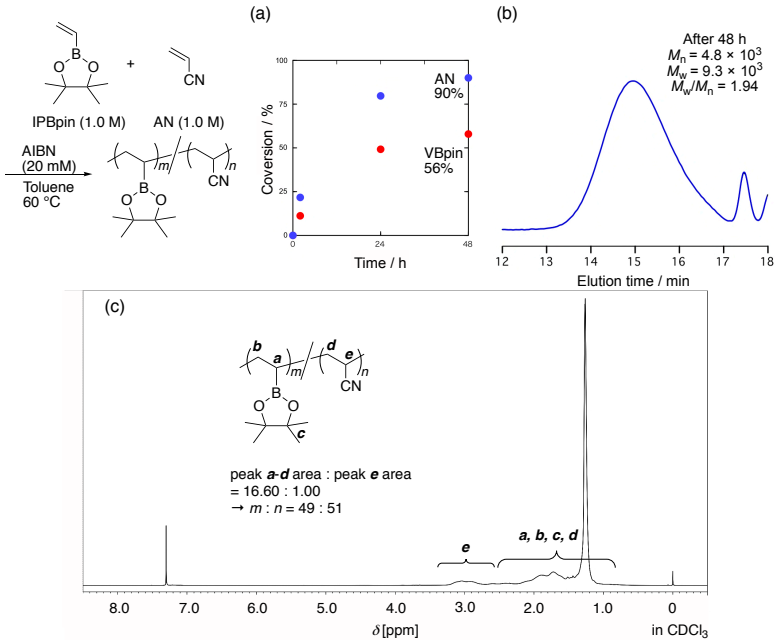

Figure S4. Radical copolymerization of VBpin with AN: (a) Time-conversion curves, (b) SEC trace of the resulting copolymer, (c) ^{1}H NMR spectrum of poly(VBpin-*co*-AN) in $CDCl_3$ after the purification.

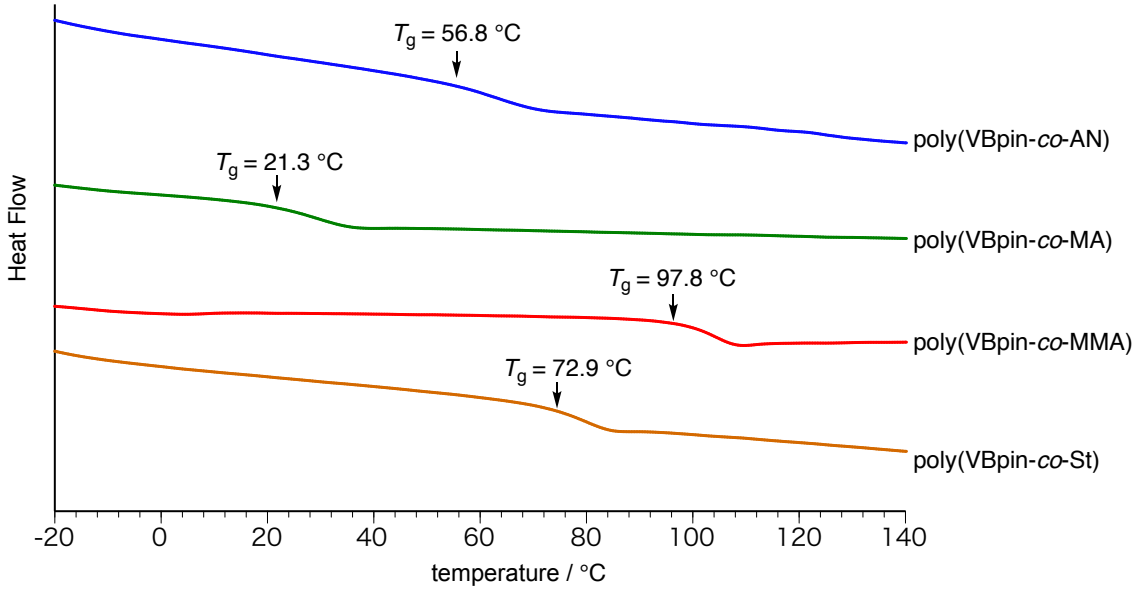

Figure S5. DSC curves (2nd heating, 10 ˚C/min) of poly(VBpin-*co*-St), poly(VBpin-*co*-MMA), poly(VBpin-*co*-MA), and poly(VBpin-*co*-AN).

4 Determination of Monomer Reactivity Ratios

Mayo and Lewis described the copolymerization behavior of two monomers (M_1 and M_2) by the equation shown below, where $[M_1]$ is the concentration of M_1, $[M_2]$ is the concentration of M_2, r_1 and r_2 are the reactivity ratio of M_1 and M_2.[1]

$$\frac{d[M_1]}{d[M_2]} = \frac{[M_1](r_1[M_1] + [M_2])}{[M_2](r_2[M_2] + [M_1])} \qquad (1)$$

When the monomer consumptions are small enough, Mayo-Lewis equation shown above can be approximated as

$$\frac{\Delta[M_1]}{\Delta[M_2]} \fallingdotseq \frac{[M_1]_0(r_1[M_1]_0 + [M_2]_0)}{[M_2]_0(r_2[M_2]_0 + [M_1]_0)} \qquad (2)$$

where $[M_1]_0$ is the concentration of M_1 before reaction, $[M_2]_0$ is the concentration of M_2 before reaction, $\Delta[M_1]$ is the consumption of M_1 during reaction, $\Delta[M_2]$ is the consumption of M_2 during reaction.

When we define that F_1 is the composition of M_1 in the consumed monomers during reaction ($F_1 = \Delta[M_1]/(\Delta[M_1]+\Delta[M_2])$, $F_2 = \Delta[M_2]/(\Delta[M_1]+\Delta[M_2])$), and f_1 is the composition of M_1 in monomer feed before reaction ($f_1 = [M_1]_0/([M_1]_0+[M_2]_0)$, $f_2 = [M_2]_0/([M_1]_0+[M_2]_0)$), equation (2) can be expressed as shown below.[2]

$$F_1 = \frac{r_1 {f_1}^2 + f_1(1 - f_1)}{r_1 {f_1}^2 + 2f_1(1 - f_1) + r_2(1 - f_1)^2} \qquad (3)$$

On the basis of equation (3) and the experimental results obtained as f_1 and F_1, nonlinear least-squares fitting of f_1 versus F_1 was performed by using the Solver Function in Microsoft Office Excel 2011. Sums of the squares of the deviation were minimized by optimizing r_1 and r_2. The experimental procedure to obtain f_1 and F_1 series in each copolymerization is shown in following section.

Copolymerization of VBpin and vinyl comonomers were performed with AIBN. The sum of the concentrations of both monomers was 2000 mM, and the feed ratio of each monomer was changed ($[VBpin]_0$:$[comonomer]_0$ = 90:10, 70:30, 50:50, 30:70, and 10:90).

Typical procedure of the copolymerization for determination of monomer reactivity ratios is as follows: A toluene solution of AIBN (4.9 mg, 30 μmol) was placed in a Schlenk tube with a PTFE stopcock (J. Young) under Ar atmosphere. Tetralin (40.9 μL, 39.7 mg, 300 μmol, internal standard), VBpin (257 μL, 231 mg, 1.5 mmol), St (172 μL, 156 mg, 1.5 mmol) and toluene (538 μL) were then added at room temperature (5:5 feed ratio condition). The reaction mixture was placed in an oil bath at 60 °C. After 3.5 h, the solution was cooled to −25 °C to terminate the polymerization. The composition ratio [$F = DP_{\mathrm{VBpin}}/(DP_{\mathrm{VBpin}} + DP_{\mathrm{comonomer}})$] was determined from the monomer conversion ratio [Conv.(VBpin)/(Conv.(VBpin) + Conv.(comonomer))] by ^{1}H NMR ($CDCl_3$) with tetralin as an internal standard. The actual monomer feed ratio [$f = [\mathrm{VBpin}]_0/([\mathrm{VBpin}]_0 + [\mathrm{comonomer}]_0$) was also determined by ^{1}H NMR spectrum (before heating). The obtained series of f_1 and F_1 were used to determine r_1 and r_2 on the basis of equation (3) through non-linear least squares method as mentioned above, affording monomer reactivity ratios shown in the main text. The monomer conversions of each copolymerization are summarized in following tables.

Table S1. Free radical copolymerization of VBpin (M_1) with St (M_2) for determination of the monomer reactivity ratios [a)]

f [b)]	Time (h)	Conv.$_{M1}$ (%) [c)]	Conv.$_{M2}$ (%) [c)]	F [d)]
0.09	1.5	6.5	7.7	0.08
0.30	3.5	4.7	15.7	0.11
0.51	3.5	3.6	16.1	0.19
0.70	3	3.9	14.9	0.38
0.90	3	3.6	14.0	0.71

a) $[M_1 + M_2]_0/[\mathrm{AIBN}]_0$ = 2000/20 mM in toluene at 60 °C. b) Actual monomer feed ratio ($f = [M_1]_0/([M_1]_0 + [M_2]_0)$ determined by ^{1}H NMR. c) Determined by ^{1}H NMR. d) Calculated from f, Conv.$_{M1}$ and Conv.$_{M2}$.

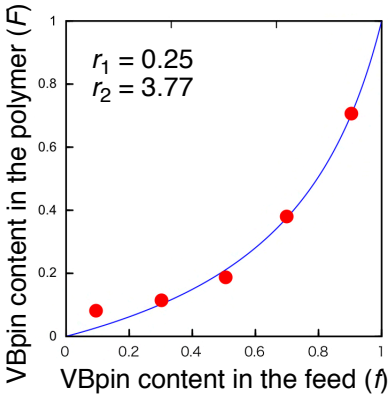

Figure S6. Copolymer–composition curve for copolymerization of VBpin (M_1) and St (M_2).

Table S2. Free radical copolymerization of VBpin (M_1) with MA (M_2) for determination of the monomer reactivity ratios [a)]

f [b)]	Time (min)	Conv.$_{M1}$ (%) [c)]	Conv.$_{M2}$ (%) [c)]	F [d)]
0.10	10	3.4	7.5	0.05
0.31	10	5.1	9.2	0.20
0.52	10	4.8	17.4	0.23
0.74	10	3.2	1.5	0.38
0.92	10	4.8	14.9	0.79

a) $[M_1 + M_2]_0/[AIBN]_0$ = 2000/20 mM in toluene at 60 °C. b) Actual monomer feed ratio (f = $[M_1]_0/([M_1]_0 + [M_2]_0)$ determined by ^{1}H NMR. c) Determined by ^{1}H NMR. d) Calculated from f, Conv.$_{M1}$ and Conv.$_{M2}$.

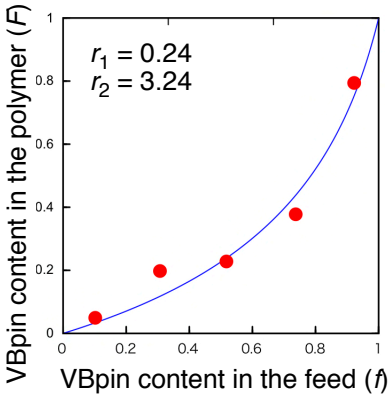

Figure S7. Copolymer–composition curve for copolymerization of VBpin (M_1) with MA (M_2).

Table S3. Free radical copolymerization of VBpin (M_1) with MMA (M_2) for determination of the monomer reactivity ratios [a)]

f [b)]	Time (min)	Conv.$_{M1}$ (%) [c)]	Conv.$_{M2}$ (%) [c)]	F [d)]
0.10	15	8.5	6.0	0.10
0.31	20	2.3	9.3	0.12
0.50	20	2.6	12	0.31
0.72	20	1.7	9.8	0.50
0.92	15	3.2	5.5	0.86

a) $[M_1 + M_2]_0/[AIBN]_0 = 2000/20$ mM in toluene at 60 °C. b) Actual monomer feed ratio ($f = [M_1]_0/([M_1]_0 + [M_2]_0)$ determined by ^{1}H NMR. c) Determined by ^{1}H NMR. d) Calculated from f, Conv.$_{M1}$ and Conv.$_{M2}$.

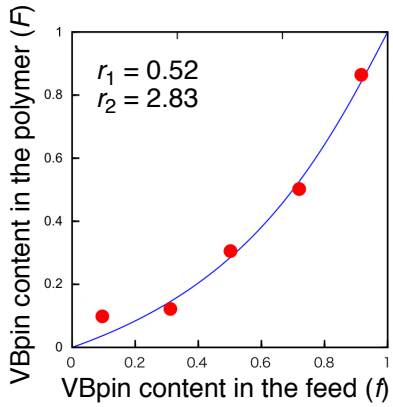

Figure S8. Copolymer−composition curve for copolymerization of VBpin (M_1) with MMA (M_2).

Table S4. Free radical copolymerization of VBpin (M_1) with AN (M_2) for determination of the monomer reactivity ratios [a)]

f [b)]	Time (min)	Conv.$_{M1}$ (%) [c)]	Conv.$_{M2}$ (%) [c)]	F [d)]
0.12	15	4.1	15.9	0.03
0.37	15	2.7	7.1	0.19
0.54	45	0.8	7.4	0.33
0.74	15	0.9	16.7	0.40
0.92	15	4.0	26.2	0.65

a) $[M_1 + M_2]_0/[AIBN]_0 = 2000/20$ mM in toluene at 60 °C. b) Actual monomer feed ratio ($f = [M_1]_0/([M_1]_0 + [M_2]_0)$ determined by ^{1}H NMR. c) Determined by ^{1}H NMR. d) Calculated from f, Conv.$_{M1}$ and Conv.$_{M2}$.

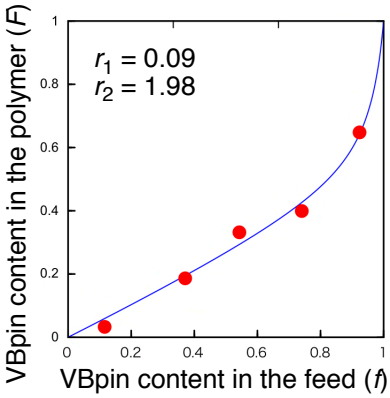

Figure S9. Copolymer–composition curve for copolymerization of VBpin (M_1) with AN (M_2).

5 DFT-based investigation for the behavior of VBpin as a conjugated monomer

The Gaussian 16A.03 program package[3] was used for computation. The density functional theory (DFT) was applied for the optimization of the structures and vibrational analysis at (U)B3LYP/6-31G* level.

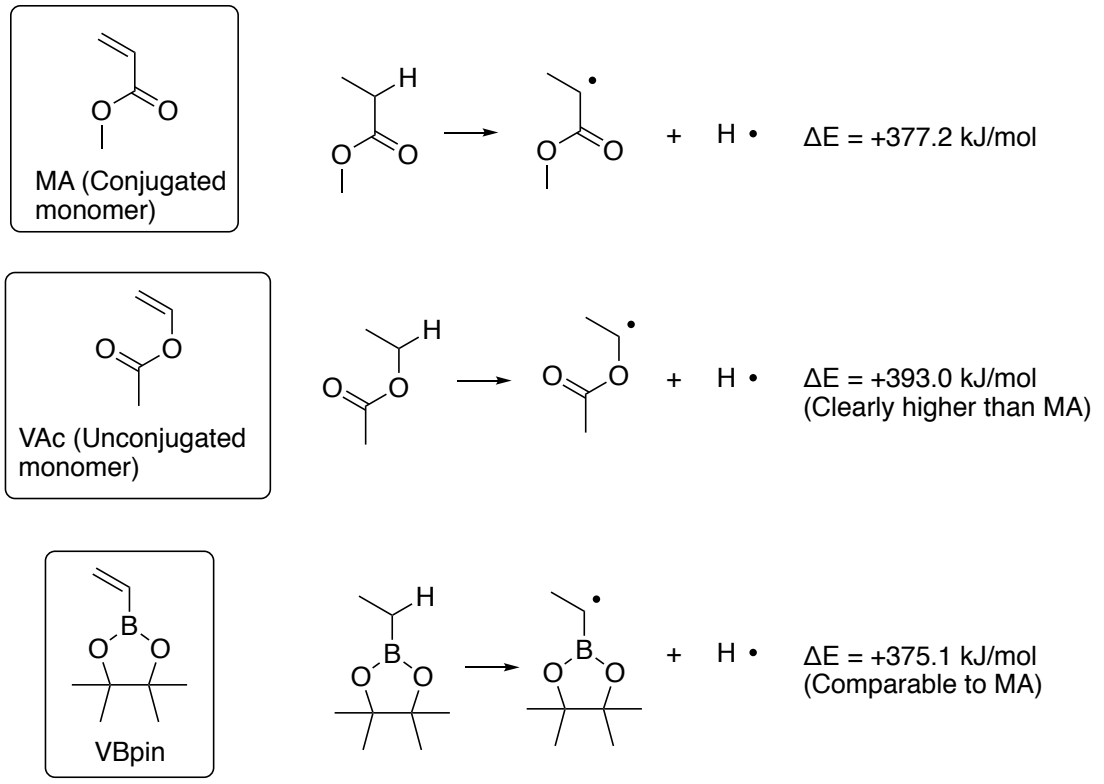

Figure S10. DFT-based estimation of radical stabilization by the pendant in MA, VAc, and VBpin based on the C-H bond dissociation energy for model compounds [(U)B3LYP/6-31g(d)].

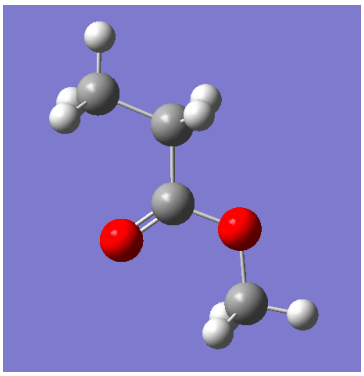

Standard orientation:

Center Number	Atomic Number	Atomic Type	Coordinates (Angstroms) X	Y	Z
1	6	0	2.482917	0.111372	0.000246
2	1	0	2.520286	0.758273	-0.881243
3	1	0	3.373406	-0.525625	0.000316
4	1	0	2.519867	0.757890	0.882038
5	6	0	1.216682	-0.742668	-0.000238
6	6	0	-0.052189	0.088344	-0.000094
7	1	0	1.181012	-1.406452	-0.873743
8	1	0	1.180790	-1.407176	0.872701
9	8	0	-1.148653	-0.706157	0.000089
10	8	0	-0.105803	1.298973	-0.000159
11	6	0	-2.408027	-0.015591	0.000109
12	1	0	-2.503028	0.613371	0.889515
13	1	0	-2.502719	0.613992	-0.888884
14	1	0	-3.170263	-0.795544	-0.000276

Sum of electronic and thermal Energies= -307.576676

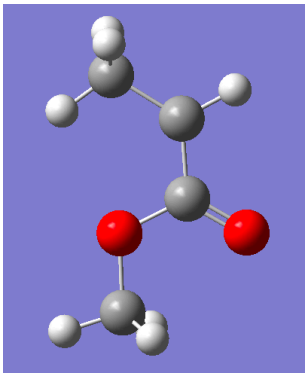

Center Number	Atomic Number	Atomic Type	Coordinates (Angstroms) X	Y	Z
1	6	0	-2.238696	-0.694611	-0.000001
2	1	0	-1.650618	-1.613874	0.000093
3	1	0	-2.901586	-0.701675	-0.878383
4	1	0	-2.901738	-0.701579	0.878265
5	6	0	-1.373172	0.514608	0.000006
6	6	0	0.075637	0.520276	0.000001
7	1	0	-1.824248	1.502158	0.000002
8	8	0	0.617097	-0.731305	0.000002
9	8	0	0.756192	1.538764	-0.000003
10	6	0	2.048941	-0.768984	-0.000001
11	1	0	2.450119	-0.272826	-0.888574
12	1	0	2.450123	-0.272814	0.888564
13	1	0	2.315378	-1.826802	0.000006

Sum of electronic and thermal Energies= -306.934149

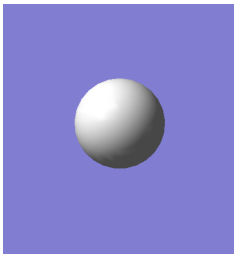

Center Number	Atomic Number	Atomic Type	Coordinates (Angstroms) X	Y	Z
1	1	0	0.000000	0.000000	0.000000

Sum of electronic and thermal Energies= -0.498857

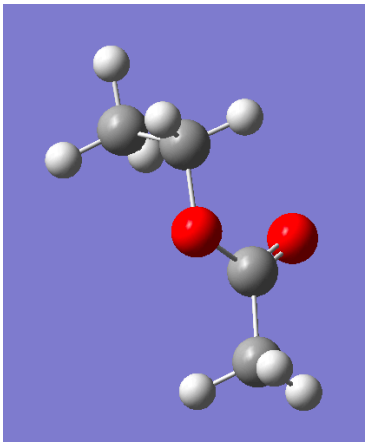

Center Number	Atomic Number	Atomic Type	Coordinates (Angstroms) X	Y	Z
1	6	0	2.182305	0.093669	0.632853
2	1	0	2.248930	-0.746945	1.331435
3	1	0	1.724523	0.944927	1.144521

4	1	0	3.199250	0.376912	0.337479
5	6	0	1.373535	-0.287975	-0.598002
6	1	0	1.827916	-1.127187	-1.130806
7	8	0	0.055234	-0.765362	-0.237237
8	1	0	1.267251	0.559841	-1.279235
9	6	0	-0.901774	0.176148	-0.058174
10	8	0	-0.715490	1.366632	-0.187286
11	6	0	-2.216928	-0.467470	0.317043
12	1	0	-2.525661	-1.175921	-0.458519
13	1	0	-2.105933	-1.032577	1.248478
14	1	0	-2.977058	0.304554	0.440514

Sum of electronic and thermal Energies= -307.580890

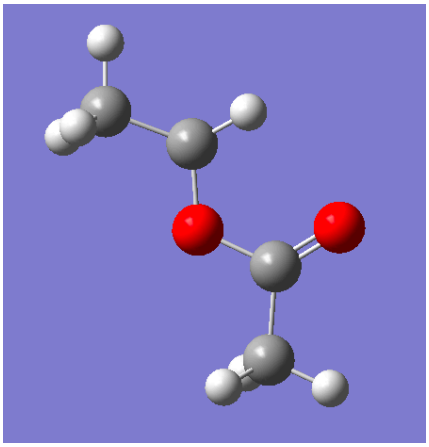

Center Number	Atomic Number	Atomic Type	Coordinates (Angstroms) X	Y	Z
1	6	0	-2.618597	-0.312464	0.062652
2	1	0	-3.447183	0.360102	-0.180613
3	1	0	-2.763509	-0.656000	1.101897

4	1	0	-2.693613	-1.199460	-0.579351
5	6	0	-1.325184	0.386359	-0.131108
6	8	0	-0.211791	-0.425570	-0.059967
7	1	0	-1.153850	1.439250	0.053614
8	6	0	1.025427	0.162137	0.004440
9	8	0	1.193193	1.358702	0.036013
10	6	0	2.103630	-0.891838	0.020261
11	1	0	1.931320	-1.604378	0.833336
12	1	0	2.088792	-1.457538	-0.917910
13	1	0	3.075168	-0.412197	0.143188

Sum of electronic and thermal Energies= -306.932343

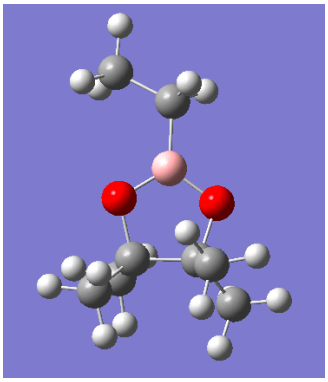

Center Number	Atomic Number	Atomic Type	Coordinates (Angstroms) X	Y	Z
1	8	0	0.146568	-1.291930	-0.396635
2	5	0	1.146260	-0.419402	-0.031854
3	6	0	-1.126278	-0.685945	-0.037433
4	8	0	0.663283	0.810202	0.349679
5	6	0	-0.758668	0.847767	0.042367
6	6	0	-2.155475	-1.055293	-1.104463

7	6	0	2.672947	-0.801304	-0.035498
8	6	0	-1.533618	-1.287599	1.314796
9	6	0	-0.897304	1.580264	-1.299316
10	6	0	-1.470108	1.633522	1.142643
11	1	0	-1.573136	-2.377179	1.219923
12	1	0	-0.805773	-1.043794	2.095254
13	1	0	-2.518810	-0.933692	1.636620
14	1	0	-1.823671	-0.765084	-2.103880
15	1	0	-2.311279	-2.138921	-1.103337
16	1	0	-3.119566	-0.574451	-0.902239
17	1	0	-1.269653	1.216250	2.132012
18	1	0	-1.119301	2.670549	1.137591
19	1	0	-2.554009	1.642025	0.979527
20	1	0	-0.435825	2.568825	-1.212575
21	1	0	-0.387281	1.039628	-2.102907
22	1	0	-1.946906	1.713329	-1.582205
23	1	0	2.852939	-1.473836	0.818063
24	1	0	2.877637	-1.419372	-0.921086
25	6	0	3.643378	0.388841	0.028624
26	1	0	3.527774	1.044394	-0.842248
27	1	0	3.459057	1.002081	0.917399
28	1	0	4.688451	0.058569	0.058689

Sum of electronic and thermal Energies= -490.251279

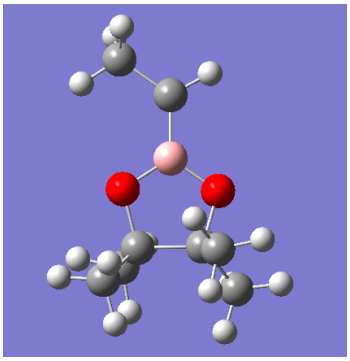

Center Number	Atomic Number	Atomic Type	Coordinates (Angstroms) X	Y	Z
1	6	0	3.760613	0.266192	0.126608
2	1	0	3.367452	1.247995	0.406271
3	1	0	4.430913	0.400456	-0.737502
4	1	0	4.404162	-0.089923	0.946934
5	6	0	2.669314	-0.709051	-0.174816
6	5	0	1.174134	-0.387403	-0.098893
7	1	0	2.985505	-1.711147	-0.465888
8	8	0	0.678280	0.843419	0.287498
9	8	0	0.175940	-1.290062	-0.407606
10	6	0	-0.749927	0.842669	0.021257
11	6	0	-1.088194	-0.699731	-0.002755
12	6	0	-2.160451	-1.115723	-1.008747
13	6	0	-0.945935	1.529676	-1.337903
14	6	0	-1.446989	1.645857	1.118361
15	6	0	-1.418183	-1.271895	1.383455
16	1	0	-0.502616	2.529482	-1.296541
17	1	0	-0.449757	0.973597	-2.139604
18	1	0	-2.006407	1.633028	-1.591401
19	1	0	-1.207329	1.263241	2.113028
20	1	0	-1.120689	2.689920	1.071828
21	1	0	-2.535178	1.625249	0.987931
22	1	0	-3.122487	-0.645937	-0.773308

23	1	0	-1.881436	-0.847201	-2.030138
24	1	0	-2.296141	-2.201456	-0.971597
25	1	0	-0.659811	-0.990107	2.120779
26	1	0	-2.395266	-0.930681	1.741895
27	1	0	-1.436836	-2.364320	1.319889

Sum of electronic and thermal Energies= -489.609552

6 Polymerization time-dependent composition of poly(VBpin-*co*-St)

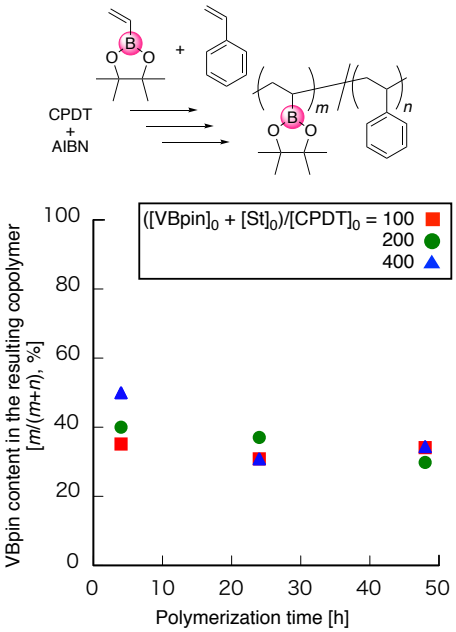

Figure S11. VBpin content [*m*/(*m*+*n*)] in the copolymer depending on the polymerization time (The calculation is based on the monomer conversion of RAFT copolymerization shown in Figure 3).

7 Synthesis of poly(VA-*co*-St) through C-B bond oxidation

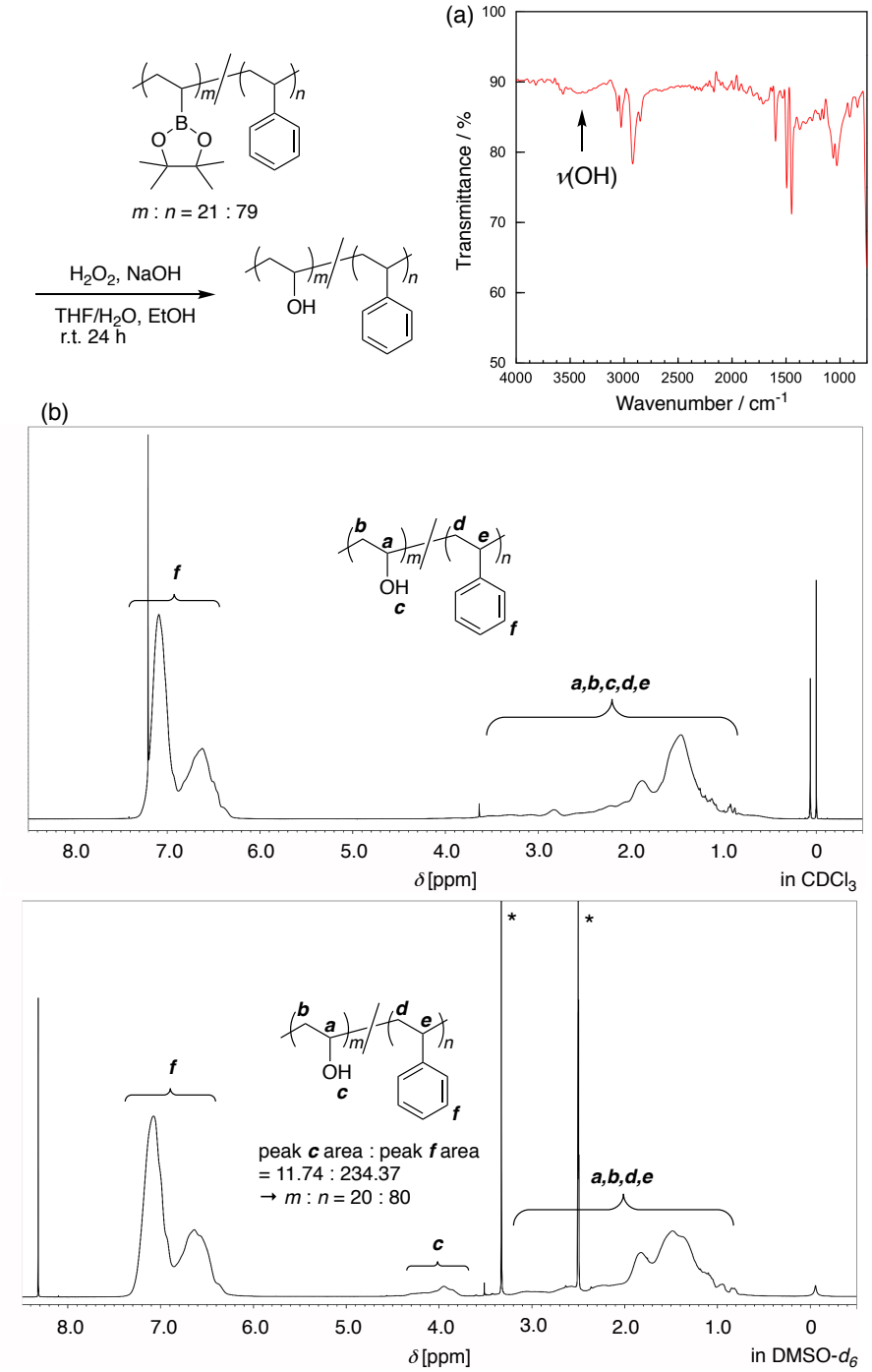

Figure S12. Oxidation of boronyl groups of poly(VBpin-*co*-St) (feed ratio in copolymerization: $[VBpin]_0/[St]_0$ = 50/50): (a) IR spectrum of resulting copolymer, (b) ^{1}H NMR spectra of the polymer in $CDCl_3$ (upper) and in DMSO-d_6 (lower).

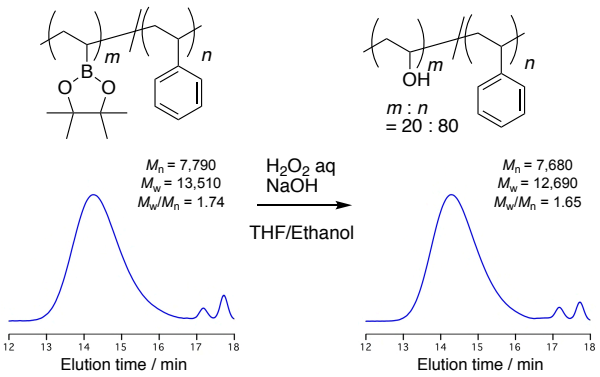

Figure S13. The comparison of SEC peak shape of poly(VA-*co*-St) with its precursor poly(VBpin-*co*-St).

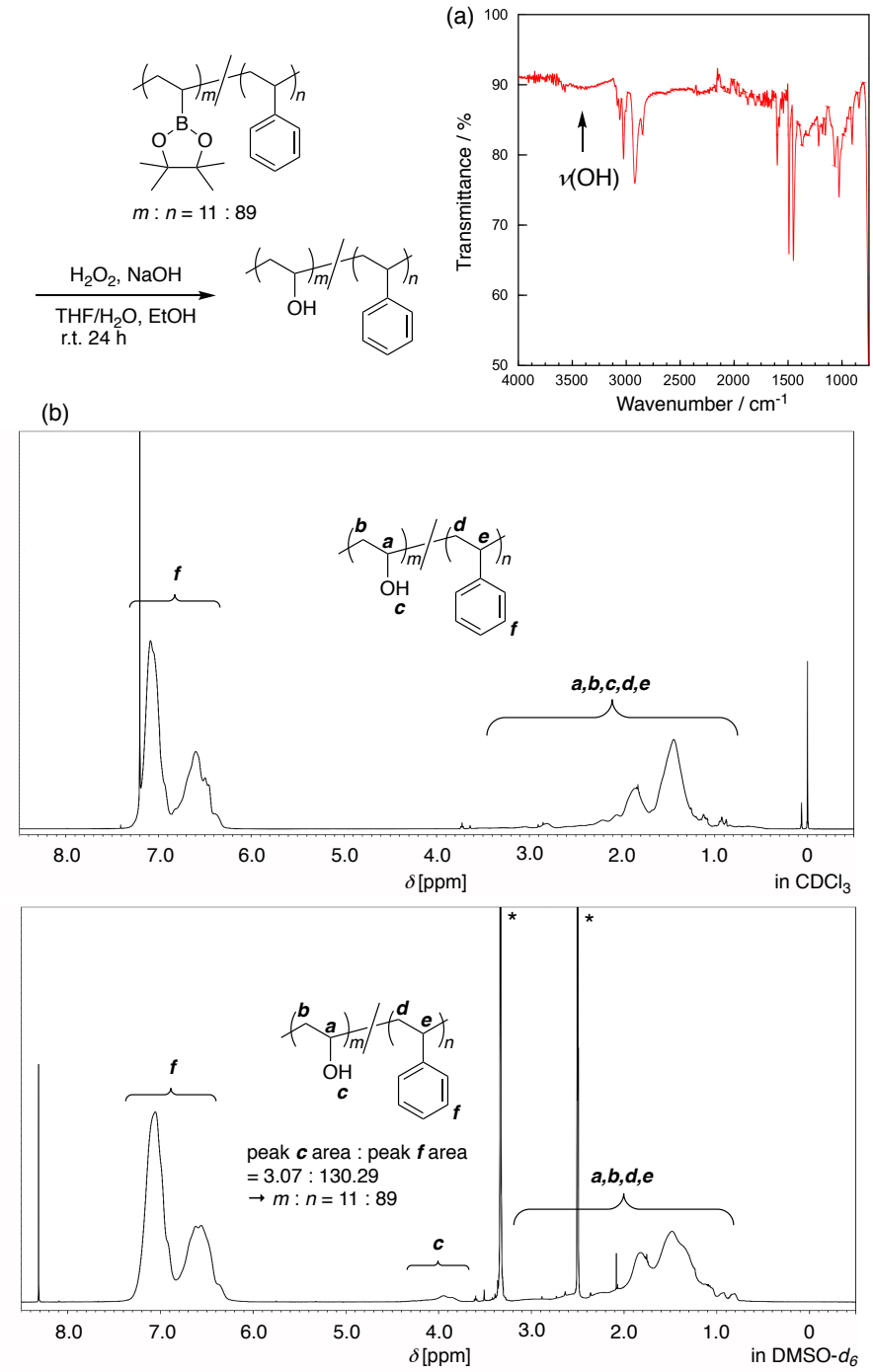

Figure S14. Oxidation of boronyl groups of poly(VBpin-*co*-St) (feed ratio in copolymerization: $[VBpin]_0/[St]_0$ = 30/70): (a) IR spectrum of the resulting copolymer, (b) ^{1}H NMR spectra of the polymer in $CDCl_3$ (upper) and in DMSO-d_6 (lower).

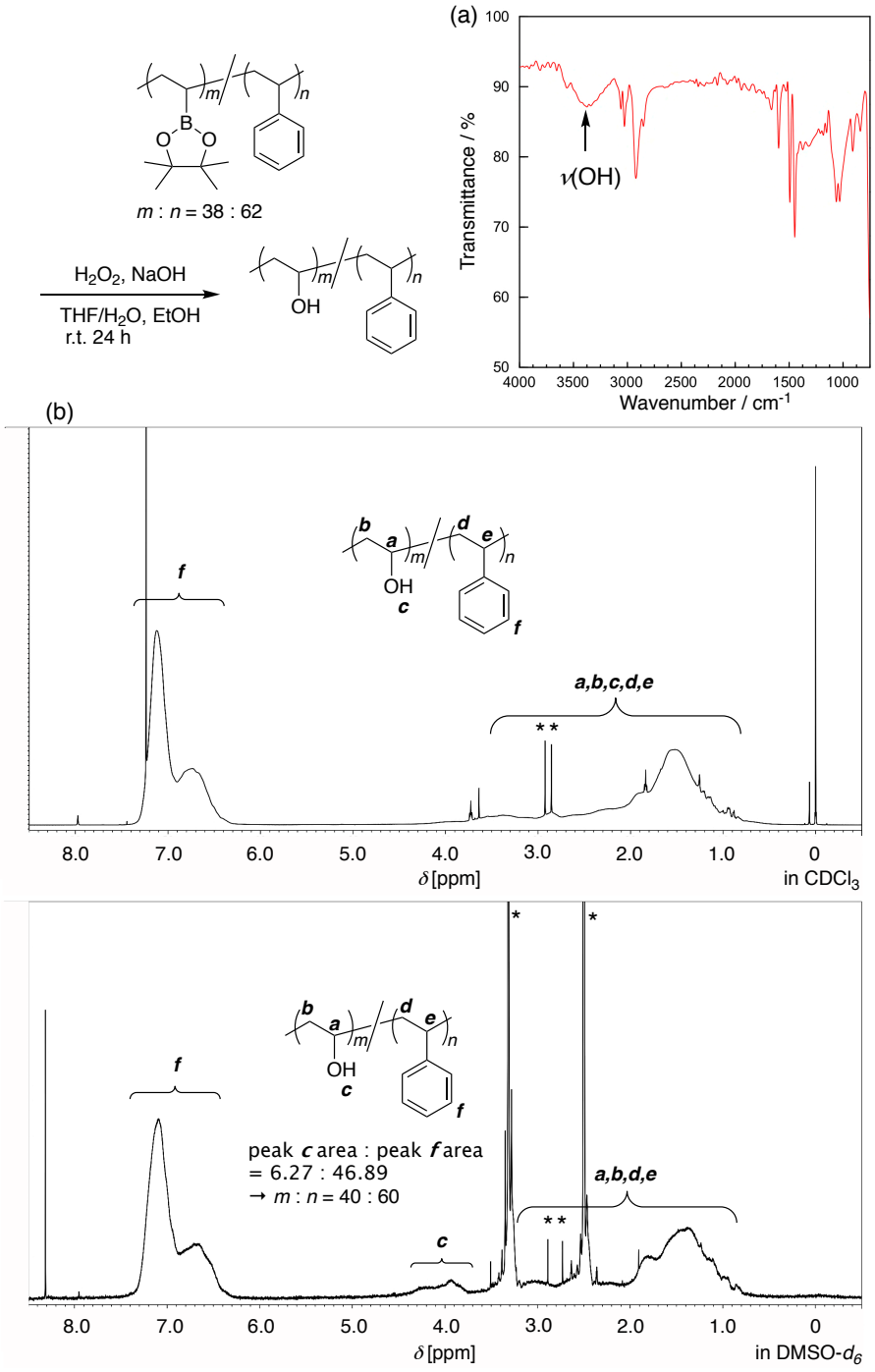

Figure S15. Oxidation of boronyl groups of poly(VBpin-*co*-St) (feed ratio in copolymerization: $[VBpin]_0/[St]_0$ = 70/30): (a) IR spectrum of the resulting copolymer, (b) ^{1}H NMR spectra of the polymer in $CDCl_3$ (upper) and in DMSO-d_6 (lower).

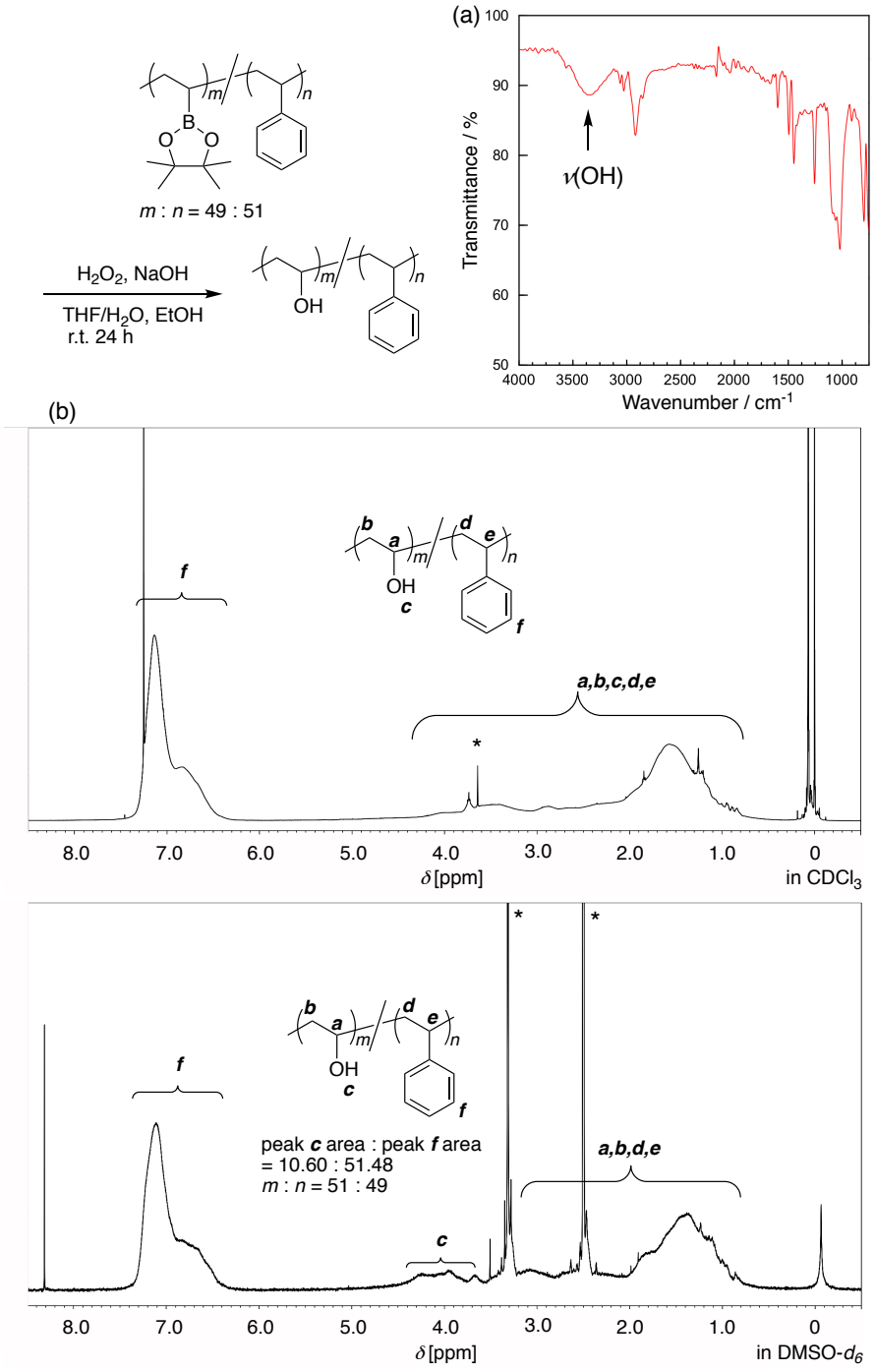

Figure S16. Oxidation of boronyl groups of poly(VBpin-*co*-St) (feed ratio in copolymerization: $[VBpin]_0/[St]_0$ = 80/20): (a) IR spectrum of the resulting copolymer, (b) ^{1}H NMR spectra of the polymer in $CDCl_3$ (upper) and in DMSO-d_6 (lower).

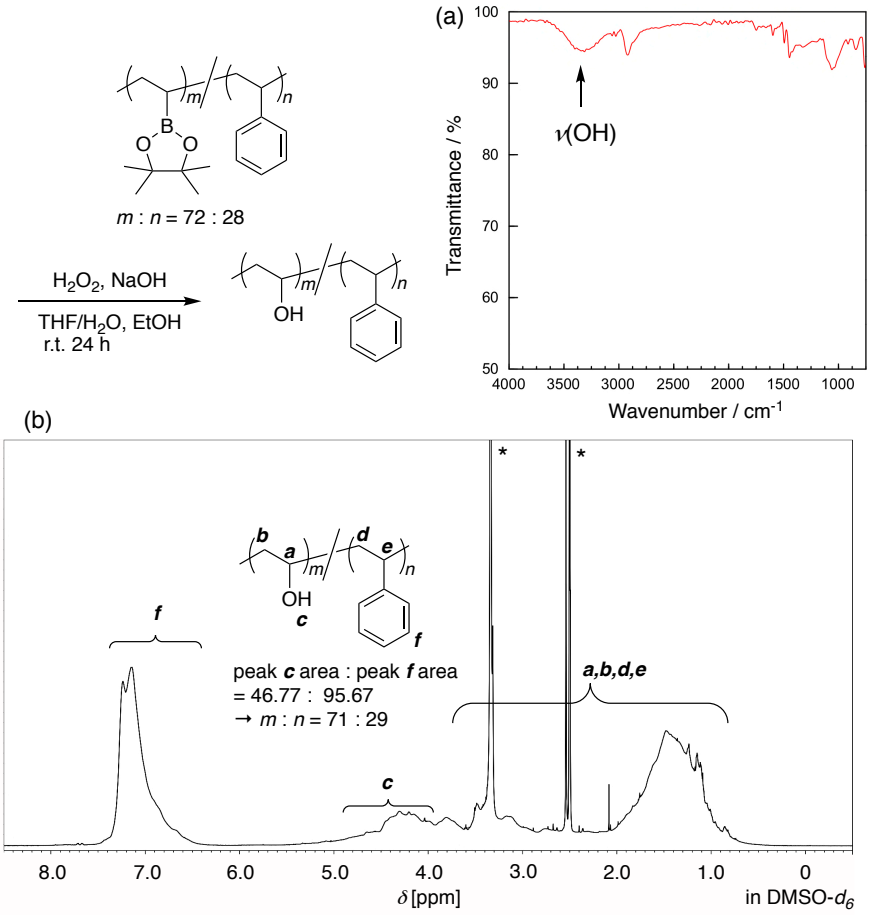

Figure S17. Oxidation of boronyl groups of poly(VBpin-*co*-St) (feed ratio in copolymerization: $[VBpin]_0/[St]_0 = 90/10$): (a) IR spectrum of the resulting copolymer, (b) ^{1}H NMR spectrum of the polymer in DMSO-d_6.

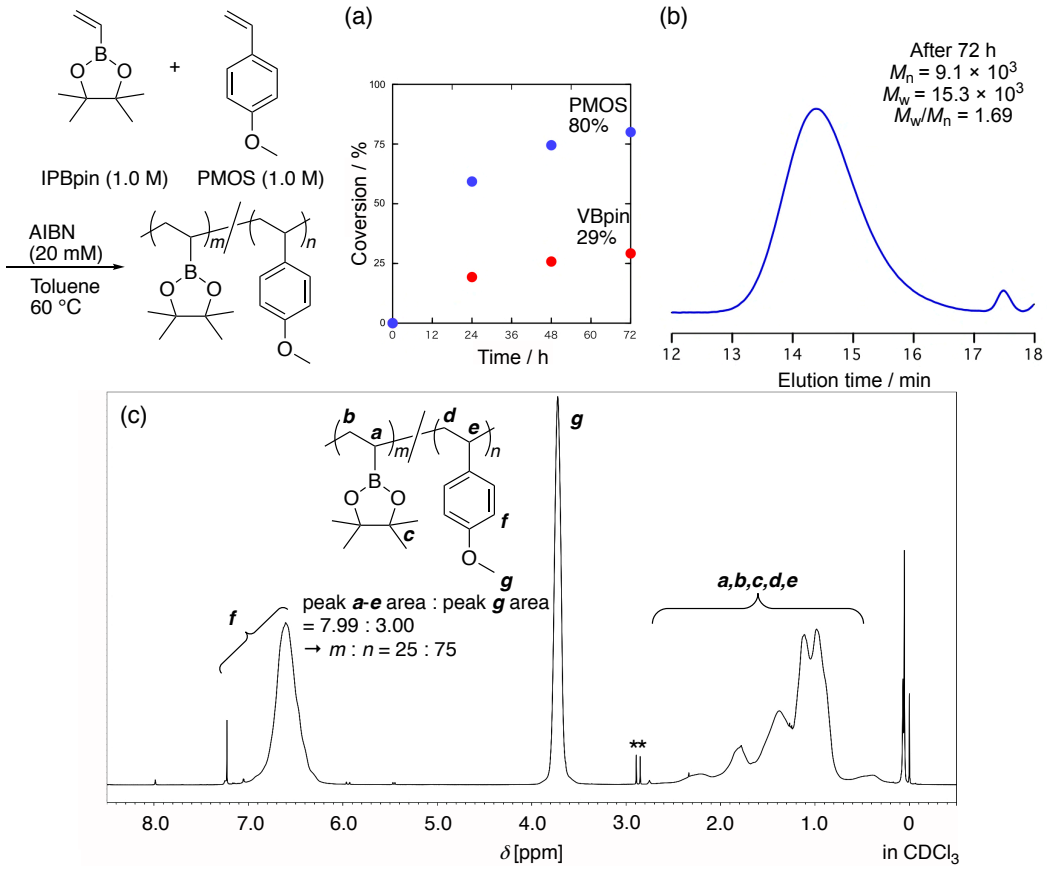

Figure S18. Radical copolymerization of VBpin with PMOS: (a) Time-conversion curves of copolymerization, (b) SEC trace of the resulting copolymer, (c) ^{1}H NMR spectrum of the polymer in $CDCl_3$ after the purification.

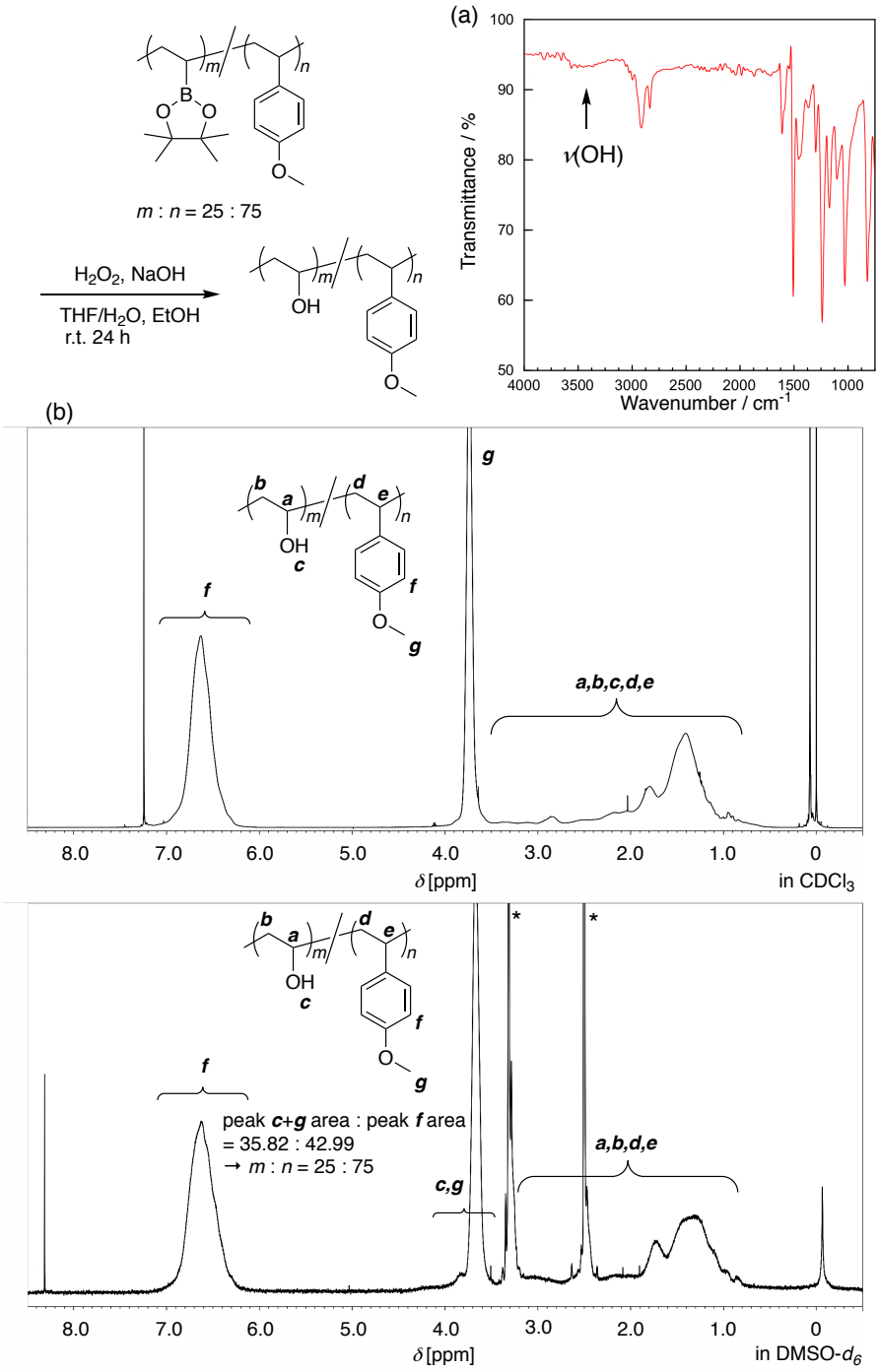

Figure S19. Oxidation of boronyl groups of poly(VBpin-*co*-PMOS): (a) IR spectrum of the resulting copolymer, (b) ^{1}H NMR spectra of the obtained copolymer in $CDCl_3$ (upper) and in DMSO-d_6 (lower).

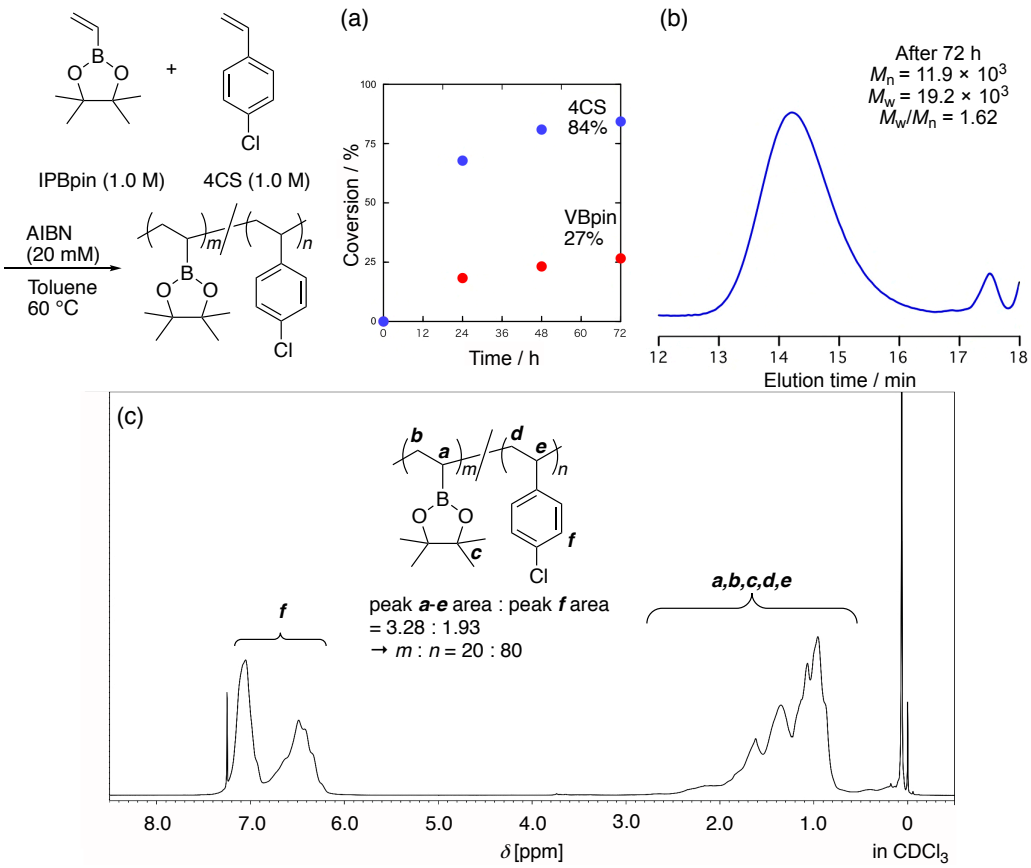

Figure S20. Radical copolymerization of VBpin with 4CS: (a) Time-conversion curves of copolymerization, (b) SEC trace of the resulting copolymer, (c) ^{1}H NMR spectrum of the polymer in $CDCl_3$ after the purification.

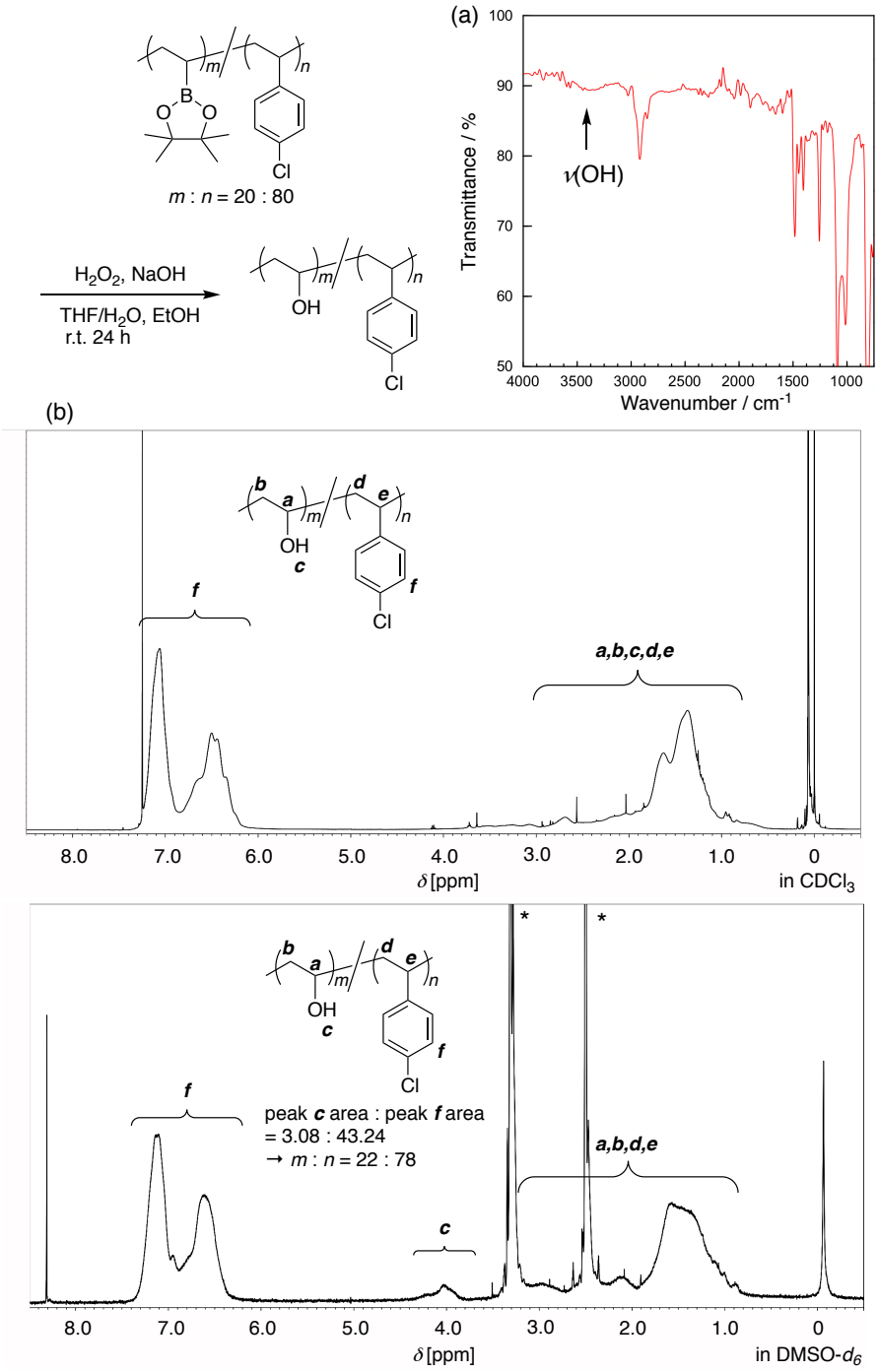

Figure S21. Oxidation of boronyl groups of poly(VBpin-*co*-4CS): (a) IR spectrum of the resulting copolymer, (b) ^{1}H NMR spectra of the polymer in $CDCl_3$ (upper) and in DMSO-d_6 (lower).

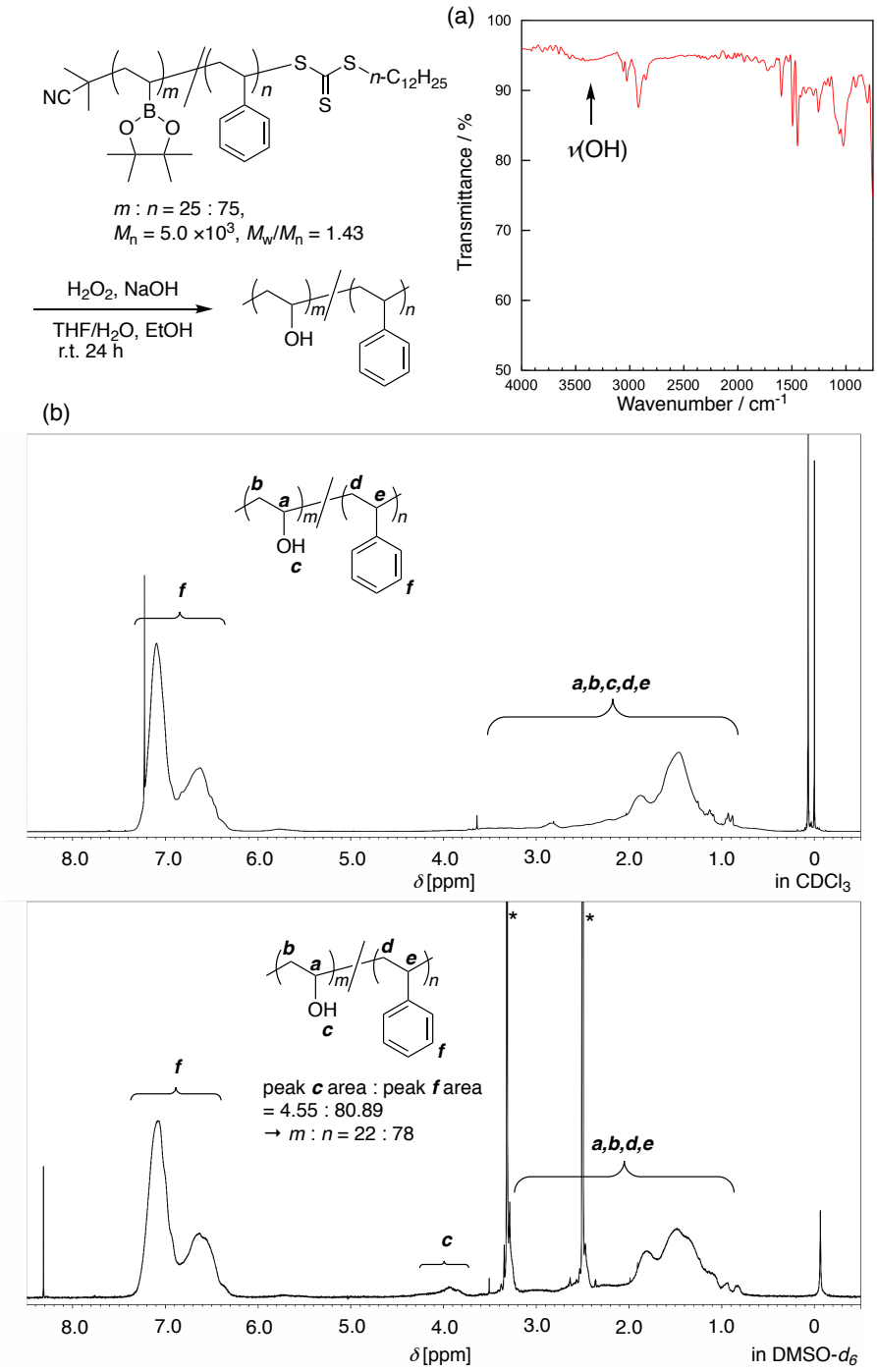

Figure S22. Oxidation of boronyl groups of poly(VBpin-*co*-St) synthesized by RAFT copolymerization [polymerization condition: ([VBpin]$_0$+[St]$_0$)/[CPDT]$_0$ = 100]: (a) IR spectrum of the resulting copolymer, (b) ^{1}H NMR spectra of the polymer in $CDCl_3$ (upper) and in DMSO-d_6 (lower).

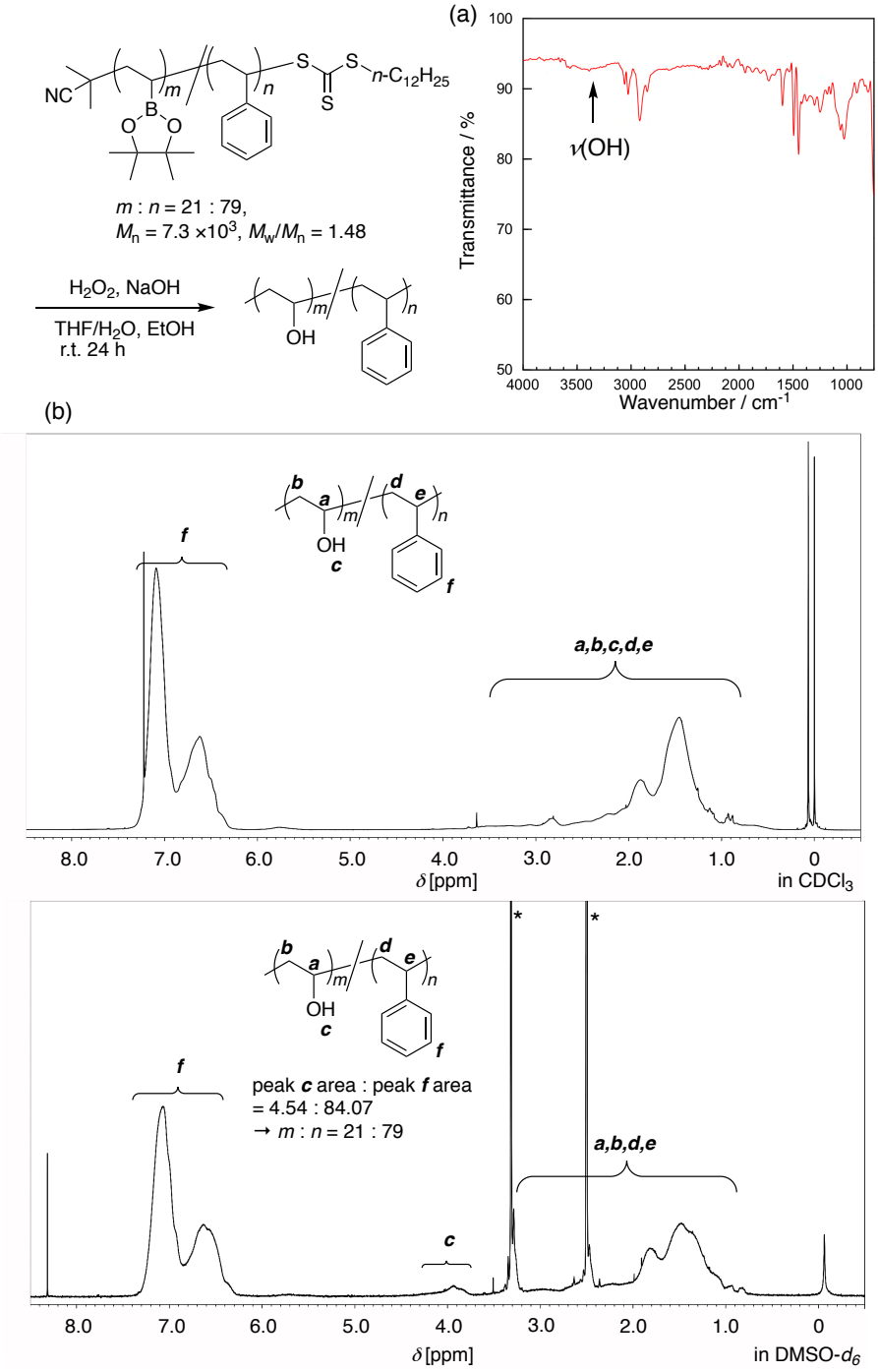

Figure S23. Oxidation of boronyl groups of poly(VBpin-*co*-St) synthesized by RAFT copolymerization [polymerization condition: ([VBpin]$_0$+[St]$_0$)/[CPDT]$_0$ = 200]: (a) IR spectrum of the resulting copolymer, (b) ^{1}H NMR spectra of the polymer in $CDCl_3$ (upper) and in DMSO-d_6 (lower).

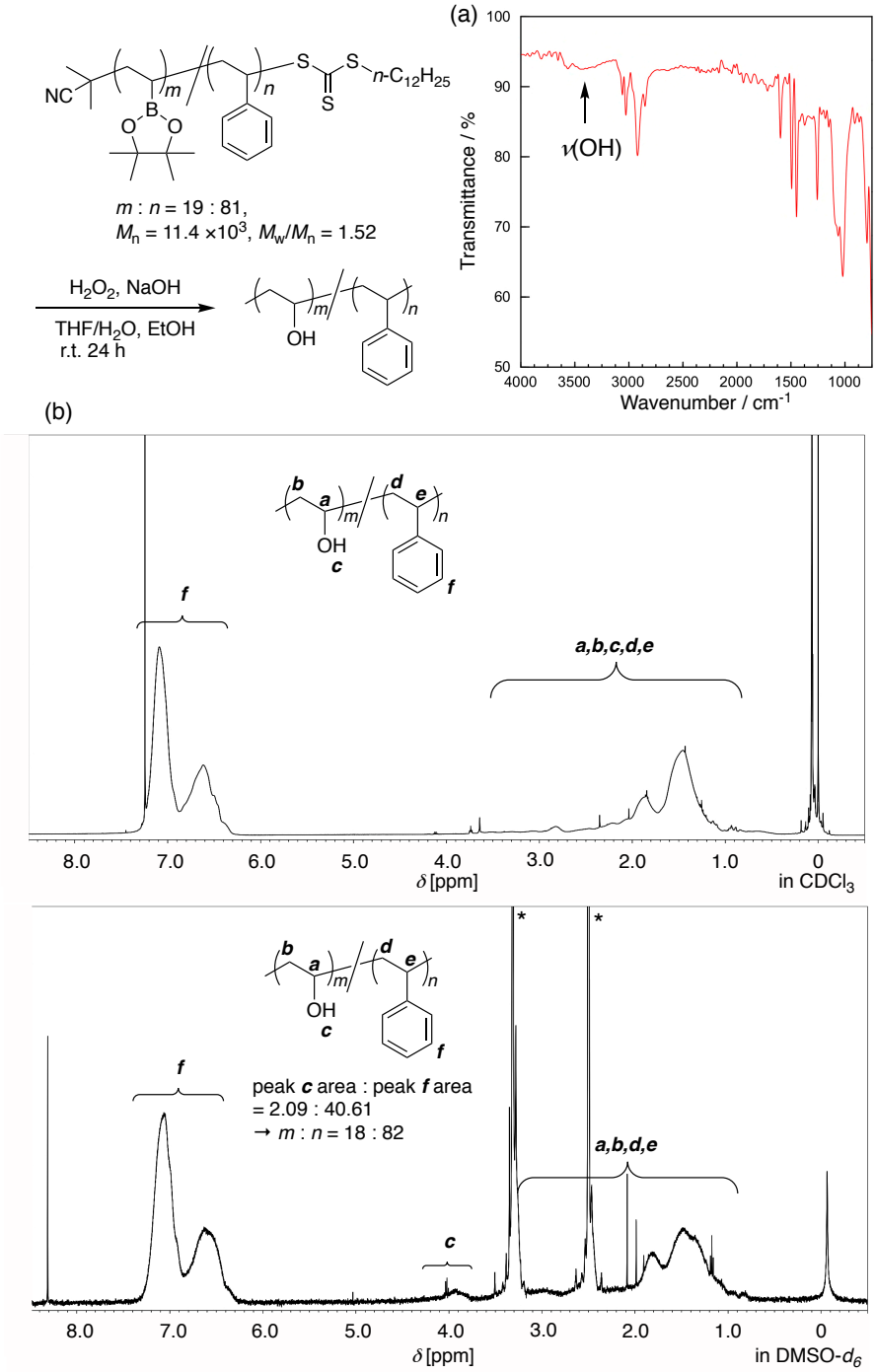

Figure S24. Oxidation of boronyl groups of poly(VBpin-*co*-St) synthesized by RAFT copolymerization [polymerization condition: ($[VBpin]_0$+$[St]_0$)/$[CPDT]_0$ = 400]: (a) IR spectrum of the resulting copolymer. (b) ^{1}H NMR spectra of the polymer in $CDCl_3$ (upper) and in DMSO-d_6 (lower).

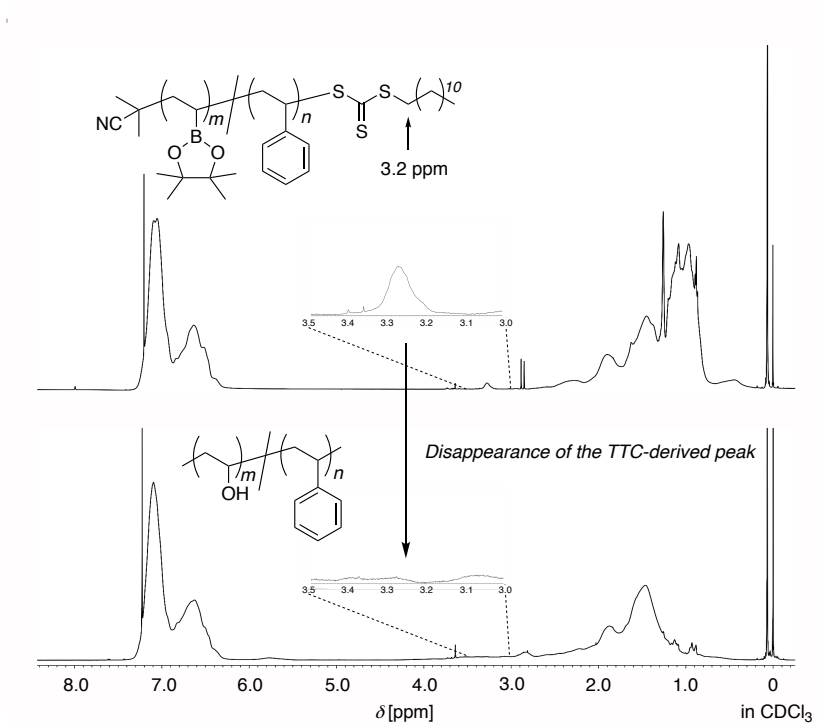

Figure S25. Change of ^{1}H NMR spectra in the oxidation of poly(VBpin-*co*-St) prepared by RAFT polymerization.

Table S5. Purification processes and yields of poly(VA-*co*-St)s for the oxidation of poly(VBpin-*co*-St)s shown in Figure 5

Entry	Purification process	Yield (wt%)
1	Dialysis (water/THF = 50/50(v/v) → 30/70 → 0/100) → Preparative GPC (Eluent: $CHCl_3$)	97
2	Dialysis (water/THF = 50/50(v/v) → 30/70 → 0/100) → Preparative GPC (Eluent: $CHCl_3$)	76
3	Dialysis (water/THF = 50/50(v/v) → 30/70 → 0/100) → Preparative GPC (Eluent: $CHCl_3$)	66
4	Dialysis (water/THF = 50/50(v/v) → 30/70 → 0/100 → 0/100)	50
5	Dialysis (water/MeOH = 50/50(v/v) → 30/70 → 0/100 → 0/100)	61
6	Dialysis (water/THF = 50/50(v/v) → 30/70 → 0/100) → Preparative GPC (Eluent: $CHCl_3$)	88
7	Dialysis (water/THF = 50/50(v/v) → 30/70 → 0/100) → Preparative GPC (Eluent: $CHCl_3$)	88
8	Dialysis (water/THF = 50/50(v/v) → 30/70 → 0/100) → Preparative GPC (Eluent: $CHCl_3$)	78
9	Dialysis (water/THF = 50/50(v/v) → 30/70 → 0/100) → Preparative GPC (Eluent: $CHCl_3$)	81
10	Dialysis (water/THF = 50/50(v/v) → 30/70 → 0/100) → Preparative GPC (Eluent: $CHCl_3$)	38

8 Visual evaluation for solubility of poly(VA-*co*-St)

The basic solubility of obtained poly(VA-*co*-St)s (unit ratio: VA/St = 11/89, 20/80, 37/63, 51/49, and 71/29) were tested in the use of cyclohexane, dichloromethane, dimethyl sulfoxide, methanol, and water as the solvent. Solvent (about 1 mL) was mixed with the polymer (about 2 mg) in a glass vial, and then allowed to stand at room temperature. After several hours, the content of the vial was checked by eye-sight to judge the solubility.

9 DSC measurement of poly(VA-*co*-St)

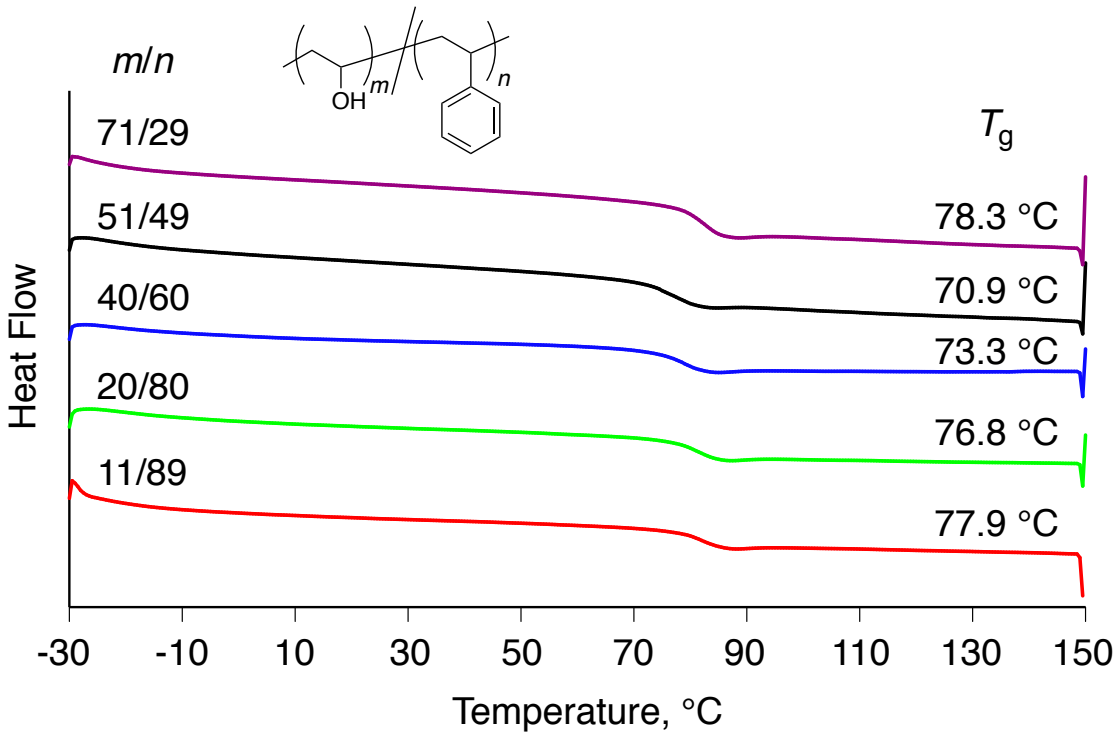

Figure S26. DSC curves (2nd heating, 10 ˚C/min) of poly(VA-*co*-St) depending on the composition ratio.

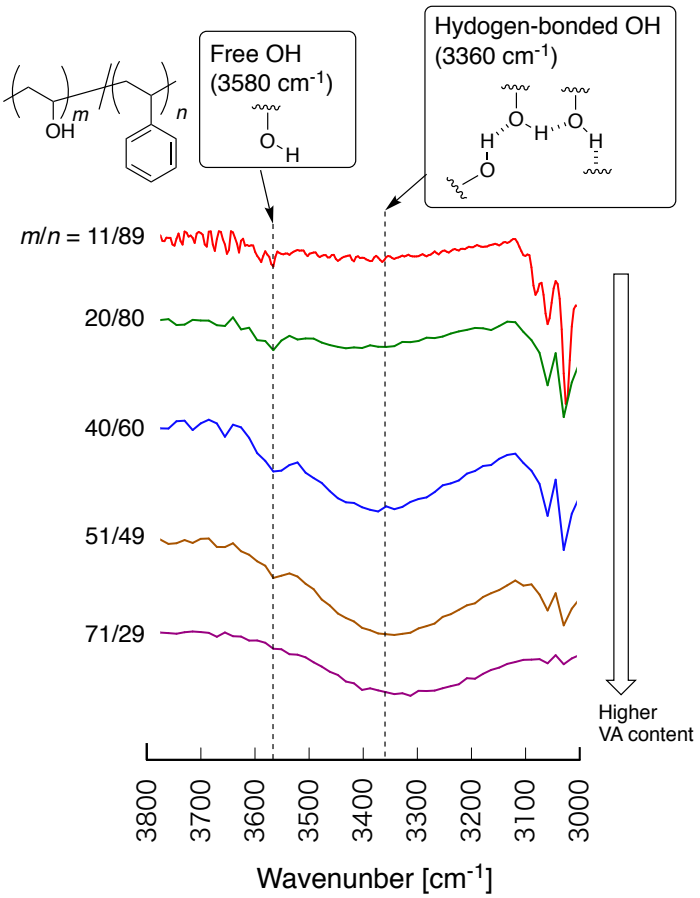

Figure S27. Change in IR spectra of poly(VA-*co*-St) depending on the VA content.

10 References

(1) Mayo, F. R.; Lewis, F. M. *J. Am. Chem. Soc.* **1944**, *66*, 1594.

(2) (a)Van Herk, A. M.; Dröge, T. *Macromol. Theory Simul.* **1997**, *6*, 1263.; (b)van de Wouw, H. L.; Awuyah, E. C.; Baris, J. I.; Klausen, R. S. *Macromolecules* **2018**, *51*, 6359.

(3) Gaussian 16, Revision A.03, M. J. Frisch, G. W. Trucks, H. B. Schlegel, G. E. Scuseria, M. A. Robb, J. R. Cheeseman, G. Scalmani, V. Barone, G. A. Petersson, H. Nakatsuji, X. Li, M. Caricato, A. V. Marenich, J. Bloino, B. G. Janesko, R. Gomperts, B. Mennucci, H. P. Hratchian, J. V. Ortiz, A. F. Izmaylov, J. L. Sonnenberg, D. Williams-Young, F. Ding, F. Lipparini, F. Egidi, J. Goings, B. Peng, A. Petrone, T. Henderson, D. Ranasinghe, V. G. Zakrzewski, J. Gao, N. Rega, G. Zheng, W. Liang, M. Hada, M. Ehara, K. Toyota, R. Fukuda, J. Hasegawa, M. Ishida, T. Nakajima, Y. Honda, O. Kitao, H. Nakai, T. Vreven, K. Throssell, J. A. Montgomery, Jr., J. E. Peralta, F. Ogliaro, M. J. Bearpark, J. J. Heyd, E. N. Brothers, K. N. Kudin, V. N. Staroverov, T. A. Keith, R. Kobayashi, J. Normand, K. Raghavachari, A. P. Rendell, J. C. Burant, S. S. Iyengar, J. Tomasi, M. Cossi, J. M. Millam, M. Klene, C. Adamo, R. Cammi, J. W. Ochterski, R. L. Martin, K. Morokuma, O. Farkas, J. B. Foresman, and D. J. Fox, Gaussian, Inc., Wallingford CT, **2016**